



Article

# On the Theoretical CO<sub>2</sub> Sequestration Potential of Pervious Concrete

Ethan Ellingboe <sup>1</sup>, Jay H. Arehart <sup>2</sup> and Wil V. Srubar III <sup>2,3,\*</sup>

<sup>1</sup> Department of Chemical and Biological Engineering, University of Colorado Boulder, Boulder, CO 80309, USA; ethan.ellingboe@colorado.edu

<sup>2</sup> Department of Civil, Environmental, and Architectural Engineering, University of Colorado Boulder, Boulder, CO 80309, USA; joseph.arehart@colorado.edu

<sup>3</sup> Materials Science and Engineering Program, University of Colorado Boulder, Boulder, CO 80309, USA

\* Correspondence: wsrubar@colorado.edu; Tel.: +1-303-492-2621

Received: 17 January 2019; Accepted: 8 March 2019; Published: 16 March 2019



**Abstract:** Pervious concrete, which has recently found new applications in buildings, is both energy- and carbon-intensive to manufacture. However, similar to normal concrete, some of the initial CO<sub>2</sub> emissions associated with pervious concrete can be sequestered through a process known as carbonation. In this work, the theoretical formulation and application of a mathematical model for estimating the carbon dioxide (CO<sub>2</sub>) sequestration potential of pervious concrete is presented. Using principles of cement and carbonation chemistry, the model related mixture proportions of pervious concretes to their theoretical in situ CO<sub>2</sub> sequestration potential. The model was subsequently employed in a screening life cycle assessment (LCA) to quantify the percentage of recoverable CO<sub>2</sub> emissions—namely, the ratio of in situ sequesterable CO<sub>2</sub> to initial cradle-to-gate CO<sub>2</sub> emissions—for common pervious concrete mixtures. Results suggest that natural carbonation can recover up to 12% of initial CO<sub>2</sub> emissions and that CO<sub>2</sub> sequestration potential is maximized for pervious concrete mixtures with (i) lower water-to-cement ratios, (ii) higher compressive strengths, (iii) lower porosities, and (iv) lower hydraulic conductivities. However, LCA results elucidate that mixtures with maximum CO<sub>2</sub> sequestration potential (i.e., mixtures with high cement contents and CO<sub>2</sub> recoverability) emit more CO<sub>2</sub> from a net-emissions perspective, despite their enhanced in situ CO<sub>2</sub> sequestration potential.

**Keywords:** pervious concrete; carbonation; CO<sub>2</sub> sequestration; life cycle assessment

## 1. Introduction

Utilization of pervious concrete has increased in recent years in applications specific to both vertical (i.e., building) and horizontal (i.e., transportation) infrastructure [1–3]. Over the past decade, pervious concrete has been applied in buildings as non-structural components, such as sound barriers, insulation panels, and living walls—applications that take advantage of its favorable acoustic, thermal, and hydraulic conductivity properties. In more conventional horizontal pavement applications, the use of pervious concrete has been shown to reduce the quantity and improve the quality of stormwater runoff [4–6] in urban environments.

Pervious concrete consists of coarse aggregate, ordinary portland cement (OPC), and water, while water-reducing admixtures are commonly added to ensure proper workability and other fresh- and hardened-state characteristics [4]. The absence of fine aggregate in pervious concrete yields a porous structure, enabling water and air to permeate through the material. In pavement applications, infiltration of water through the surface significantly reduces stormwater runoff volume, which lowers the potential to pollute water supplies, mitigates downstream erosion caused by flooding, and may

improve road safety by reducing the risk of hydroplaning [4,7–9]. These benefits have led green building rating systems, such as the United States Green Building Council's Leadership in Energy and Environmental Design (LEED) building certification program, to promote the use of pervious concrete as a low-impact site development strategy.

Important material properties of pervious concrete (i.e., compressive strength, porosity, hydraulic conductivity) are governed primarily by the size of the coarse aggregate and the thickness of the cement paste that binds them together [4,10–12]. In general, paste thickness increases with cement content, which results in decreased porosity and hydraulic conductivity but improved compressive strength [10]. Contrastingly, pore sizes, on average, increase with the size of coarse aggregate [4,11], resulting in increased pore connectivity and hydraulic conductivity but decreased compressive strength [11–13].

### 1.1. CO<sub>2</sub> Emissions and CO<sub>2</sub> Sequestration

The manufacture, use, and disposal of OPC, a primary constituent of pervious concrete, has significant environmental impacts. While the production of OPC currently accounts for  $\approx$  5% of global carbon dioxide (CO<sub>2</sub>) emissions [14,15], previous research has shown that the natural carbonation process of cementitious materials can sequester—and, thus, recover—non-trivial quantities of CO<sub>2</sub> both during and after their in-service lifetime [16–18].

Simple predictive models enable quantification of the CO<sub>2</sub> sequestration potential of cementitious materials, allowing the positive effects of carbonation to be included in life cycle assessments (LCAs). LCA is a tool used by architects and engineers to better understand the environmental impacts of building products and manufacturing processes. Similar mathematical models have been used to analyze normal OPC concrete with results indicating that a significant percentage of initial CO<sub>2</sub> emitted during OPC production is permanently sequestered by the concrete after placement [19–22]. For example, Yang et al. [19] estimated that up to 17% of CO<sub>2</sub> emissions from concrete production could be recovered via sequestration over a 100-year period, given a 40-year service life and 60-year recycling strategy. García-Segura et al. [20] approximated that up to 47% of total CO<sub>2</sub> emissions are recaptured through sequestration if concrete is demolished, crushed, and recycled. Previously developed models apply only to regular OPC concrete mixtures or OPC concrete mixtures with supplementary cementitious material (SCM) additives [17,20,23–26]. To date, however, to the authors' knowledge, no studies have formulated a similar model for the carbonation potential of pervious concrete.

### 1.2. Scope of Work

The primary objective of this work was to formulate and implement a theoretical model for quantifying the maximum CO<sub>2</sub> sequestration potential of OPC pervious concrete mixtures. The model developed herein is based on stoichiometric proportions of hydration and carbonation chemical reactions that occur in OPC, as well as conventional proportions of pervious concrete mixtures. A broad range of pervious concrete mixtures was theoretically designed (but not fabricated) to investigate their CO<sub>2</sub> sequestration potential. Individual design aspects, such as water-to-cement (w/c) ratio, aggregate size, and design porosity, were explicitly investigated to elucidate their impact on CO<sub>2</sub> sequestration potential. The model was applied to these concrete mix designs and implemented in a screening LCA to estimate the percentage of initial cradle-to-gate CO<sub>2</sub> emissions that are recoverable by in situ CO<sub>2</sub> sequestration.

## 2. Computational Methods

### 2.1. Theoretical Formulation

To determine total sequesterable CO<sub>2</sub> for a representative volume of pervious concrete, first, the type of cement and the amount of reactive calcium hydroxide (CH) (i.e., portlandite) in the mixture were mathematically linked to the theoretical type and amount of cement hydration reaction products, including CH. Total sequesterable CO<sub>2</sub> per mass of carbonated pervious concrete was then calculated

using stoichiometric relationships of the carbonation reaction. Given that the appropriate depth of pervious concrete varies widely for different applications, a declared volumetric unit of 1 m<sup>3</sup> was selected to simplify bulk CO<sub>2</sub> sequestration calculations. The total volume of carbonated cement paste in pervious concrete was estimated using the cement content and theoretical porosity of each pervious concrete mixture. Quantification of the total sequesterable CO<sub>2</sub> through carbonation of cement paste in pervious concrete relies on the assumption that all of the cement in each pervious concrete mixture carbonates within the lifetime of the concrete. This assumption is further discussed and justified in Section 2.1.5.

### 2.1.1. Chemical and Mineral Composition of OPC

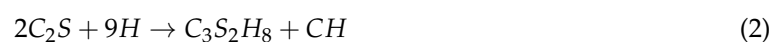
Given that Type I cement is the most widely specified cement for pervious concrete applications, only Type I cement pervious concrete mixtures are considered. Table 1 summarizes the average chemical composition and mineral content for the Type I classification of OPC as specified by the American Society of Testing and Materials (ASTM) C150 Standard [27]. In oxide notation, the primary oxides present in OPC include silicon dioxide (S), aluminum oxide (A), ferric oxide (F), calcium oxide (C), magnesium oxide (M), sulfur trioxide (Š), and sodium oxide (N), which comprise four main cement minerals, including tricalcium silicate (C<sub>3</sub>S), dicalcium silicate (C<sub>2</sub>S), tricalcium aluminate (C<sub>3</sub>A), and tetracalcium aluminoferrite (C<sub>4</sub>AF).

**Table 1.** Chemical and mineral composition of Type I OPC.

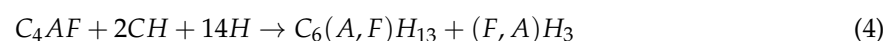
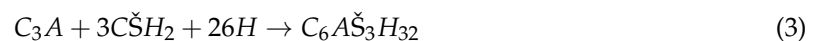
Average Oxide Composition (%)							Average Mineral (Bogue) Composition (%)					
S (SiO <sub>2</sub> )	A (Al <sub>2</sub> O <sub>3</sub> )	F (Fe <sub>2</sub> O <sub>3</sub> )	C (CaO)	M (MgO)	Š (SO <sub>3</sub> )	N (Na <sub>2</sub> O)	Other	C <sub>3</sub> S	C <sub>2</sub> S	C <sub>3</sub> A	C <sub>4</sub> AF	Other
20.5	5.4	2.6	63.9	2.1	3.0	0.61	1.9	54	18	10	8	10

### 2.1.2. Cement Hydration Reactions

According to Mehta 1986 [28], the primary hydration reactions of tricalcium silicate (C<sub>3</sub>S) and dicalcium silicate (C<sub>2</sub>S) with water (H) produce both a calcium silicate hydrate (C<sub>3</sub>S<sub>2</sub>H<sub>8</sub>) phase and CH as follows:



The primary hydration reactions of other cement minerals, namely tricalcium aluminate (C<sub>3</sub>A) and tetracalcium aluminoferrite (C<sub>4</sub>AF) yields:



where, in cement chemistry notation, CŠH<sub>2</sub> is gypsum, C<sub>6</sub>AŠ<sub>3</sub>H<sub>32</sub> is ettringite, C<sub>6</sub>(A,F)H<sub>13</sub> is calcium aluminoferrite hydrate, and (F,A)H<sub>3</sub> is aluminoferrite hydrate.

### 2.1.3. Carbonation Reaction

Previous models used to quantify CO<sub>2</sub> sequestration potential of concrete conservatively assume that CO<sub>2</sub> is sequestered by CH alone, while others incorporate the carbonation of both CH and other calcium-bearing phases [19,20,25,26,28,29]. Given the existence of dissolved CH in pore solution, in situ diffusion of CO<sub>2</sub> through the concrete matrix can initiate CH carbonation and subsequent precipitation of solid calcium carbonate (CaCO<sub>3</sub>):



where, in cement chemistry notation, CH is Ca(OH)<sub>2</sub> (calcium hydroxide),  $\bar{C}$  is CO<sub>2</sub>,  $C\bar{C}$  is CaCO<sub>3</sub>, and H is H<sub>2</sub>O (water).

The assumption that only available CH reacts via carbonation results in a conservative model prediction of sequestered CO<sub>2</sub> since the model does not account for the potential carbonation of other calcium-bearing phases (i.e., calcium silicate hydrate, or CSH). Previous studies have indicated that CSH formed in the hydration of cement paste might additionally sequester non-trivial quantities of CO<sub>2</sub> [17]. The kinetics and stoichiometry of the carbonation of CSH are not well defined, and, thus, the CO<sub>2</sub> sequestration potential of CSH in carbonated cement pastes cannot yet be readily and reliably predicted. Therefore, by assuming that only available CH participates in CO<sub>2</sub> sequestration, the model prediction likely underestimates the actual CO<sub>2</sub> sequestration potential of pervious concrete, a conservative prediction for the analysis conducted in this work.

#### 2.1.4. CO<sub>2</sub> Sequestration Potential of Cement Paste

Utilizing stoichiometric ratios of cement hydration and carbonation reactions, along with the Type I cement mineral composition, the theoretical mass of sequesterable CO<sub>2</sub> in the hydrated cement paste on a per mass basis can be computed as follows:

$$C_m = \Phi_h MW_{CH} \left( \frac{3}{2} \cdot \frac{B_{C_3S}}{MW_{C_3S}} + \frac{1}{2} \cdot \frac{B_{C_2S}}{MW_{C_2S}} - \frac{2}{1} \cdot \frac{B_{C_4AF}}{MW_{C_4AF}} \right) \left( \frac{MW_{CO_2}}{MW_{CH}} \right) \quad (6)$$

where  $C_m$  is the CO<sub>2</sub> sequestration potential (kg CO<sub>2</sub>/kg cement), and  $\Phi_h$  is the degree of hydration of the cement minerals.  $B$  and  $MW$  represent the Bogue composition and molecular weight of the cement minerals, respectively. For the purposes of this model, the degree of hydration of the cement minerals was assumed to be 100% ( $\Phi_h = 1.0$ ) to calculate the theoretical maximum of sequesterable CO<sub>2</sub> through carbonation of available CH. The stoichiometric ratios of CH produced or consumed in the hydration reactions, from Equations (1), (2) and (4), correlate to the multiplier for each mineral's contribution to CO<sub>2</sub> sequestration. Based upon full hydration of CH, Type I cement,  $C_m = 0.16$ . The conservative assumption that only CH carbonates (neglecting CSH carbonation) is in contrast to the hydration reaction being assumed to reach 100% completion. The proposed model allows for the flexibility to include other degrees of hydration and can be computed using Equation (6).

#### 2.1.5. Carbonation Depth

The bulk porosity characteristics of pervious concrete are achieved as a result of a thin layer of cement paste that surrounds individual course aggregate particles and binds them together. The porosity of pervious concrete decreases with increases in average paste thickness. The void spaces in pervious concrete allow air to diffuse through the concrete unhindered. As a result, carbonation not only proceeds from external surfaces inward but also occurs in internal pores [3]. As such, it is assumed that the cement paste layer fully carbonates in service due to (i) the immediate diffusion of air containing CO<sub>2</sub> and (ii) the small average cement paste thicknesses observed in pervious concrete mixtures [10]. This assumption enables calculation of a theoretical upper bound on the CO<sub>2</sub> sequestration potential of each pervious concrete mixture. Carbonation in the thin cement paste layers has been previously studied [17], but no mathematical models for predicting carbonation kinetics have been developed. Further, it has been demonstrated that carbonation in pervious concrete mixtures proceeds quickly in indoor environments where CO<sub>2</sub> concentrations are elevated in relation to the outdoors [3]. Carbonation degrees of 20–40% were observed in pervious concrete mixtures that were exposed to indoor environmental conditions for 2 months [3]. The typical service life of pervious concrete pavements has been conservatively estimated in the range of 7.5 to 14 years [30]. Thus, we assumed here that 100% carbonation is achievable in the typical lifetime of pervious concrete.

### 2.1.6. Total Carbonated Volume

To quantify the total carbonated volume,  $V_c$ , of the solid fraction of pervious concrete, its bulk porosity,  $\varphi$ , must be accounted for in the calculation. The total solid fraction of fully carbonated pervious concrete can be calculated according to:

$$V_c = V \cdot (1 - \varphi) \quad (7)$$

where  $V$  is the bulk volume of the pervious concrete element.

### 2.1.7. Total Mass of Sequestered CO<sub>2</sub>

Total sequesterable CO<sub>2</sub> ( $C_s$ ) of pervious concrete can be calculated as the product of the total mass of carbonated cement paste and the CO<sub>2</sub> sequestration potential ( $C_m$ ):

$$C_s = \Phi_c \cdot C_m \cdot [V_c \cdot m] \quad (8)$$

The total mass of carbonated cement paste is calculated as the term in brackets, where  $m$  is the total mass of cement per unit volume of concrete as specified in the mixture proportions. The value of  $m$  does not account for the final porosity of the pervious mixture and cannot be used to determine carbonation potential directly.  $\Phi_c$  is defined as the degree of carbonation, which was assumed to be 100% ( $\Phi_c = 1$ ) for the purposes of this study. The use of lower degrees of carbonation will result in proportionally lower predictions of CO<sub>2</sub> sequestration potential. Actual degrees of carbonation experimentally obtained in normal (non-pervious) concretes vary between 0.4 and 0.7 [30–35]. One previous study measured degrees of carbonation from 0.2 to 0.4 in pervious concrete samples exposed to indoor conditions after 60 days [3].

## 2.2. Carbonation Model Implementation

Once formulated, the model was used to investigate the effect of porosity, water-to-cement (w/c) ratio, and aggregate size on CO<sub>2</sub> sequestration potential for the mixture designs displayed in Table 2. Design porosity is defined as the desired bulk void content of the pervious concrete mixture. Mixture proportions were created according to the National Ready Mixed Concrete Association (NRMCA) pervious concrete mixture proportioning guidelines [36]. Using the accompanying spreadsheet, mixture proportions (i.e., cement content, water content, coarse aggregate content) were determined from the specified design parameters, which include void content (porosity) (15–30%), w/c ratio (0.25–0.35), and aggregate properties, such as size, absorption, dry-rodded unit density, and specific gravity. The input parameters which were maintained constant are the cement specific gravity (3.15 for Type I OPC) and compaction index (5%). The calculations conducted by the NRMCA proportioning spreadsheet were derived from recommendations for pervious concrete described in ACI 522R-10 [4]. Furthermore, the designed porosity of each mixture was used to predict the theoretical compressive strength and hydraulic conductivity of the mixture. By combining data from previous studies [4,10,37], an empirical correlation, relating porosity and compressive strength, was determined. Data are plotted in Figure 1, while Equation (9) describes the linear relationship. Recent research has shown that a difference of 3–15% between design vs. actual porosity of pervious concrete can be observed [38]. Given that this study explicitly considers a large range of design porosities, the CO<sub>2</sub> sequestration potential of as-built pervious concrete materials could be determined from this same modeling approach.

**Table 2.** Mixture proportion of pervious concrete design using NRMCA guidelines.

w/c	Aggregate Size [mm]	Component	Design Porosity						
			15.0%	17.5%	20.0%	22.5%	25.0%	27.5%	30.0%
0.25	9.54	Cement	572	528	484	440	396	352	308
		Water	143	132	121	110	99	88	77
		CA <sup>1</sup>	1349	1349	1349	1349	1349	1349	1349
	6.35	Cement	553	508	465	421	377	333	288
		Water	138	127	116	105	94	83	72
		CA <sup>1</sup>	1383	1383	1383	1383	1383	1383	1383
0.3	9.54	Cement	526	485	445	405	364	323	283
		Water	158	145	133	121	109	97	85
		CA <sup>1</sup>	1349	1349	1349	1349	1349	1349	1349
	6.35	Cement	508	468	427	387	346	306	265
		Water	152	140	128	116	104	92	79
		CA <sup>1</sup>	1383	1383	1383	1383	1383	1383	1383
0.35	9.54	Cement	486	449	412	374	336	299	262
		Water	170	157	144	131	118	105	91
		CA <sup>1</sup>	1349	1349	1349	1349	1349	1349	1349
	6.35	Cement	470	432	395	358	320	283	245
		Water	164	151	138	125	112	99	86
		CA <sup>1</sup>	1383	1383	1383	1383	1383	1383	1383

<sup>1</sup> CA = coarse aggregate.

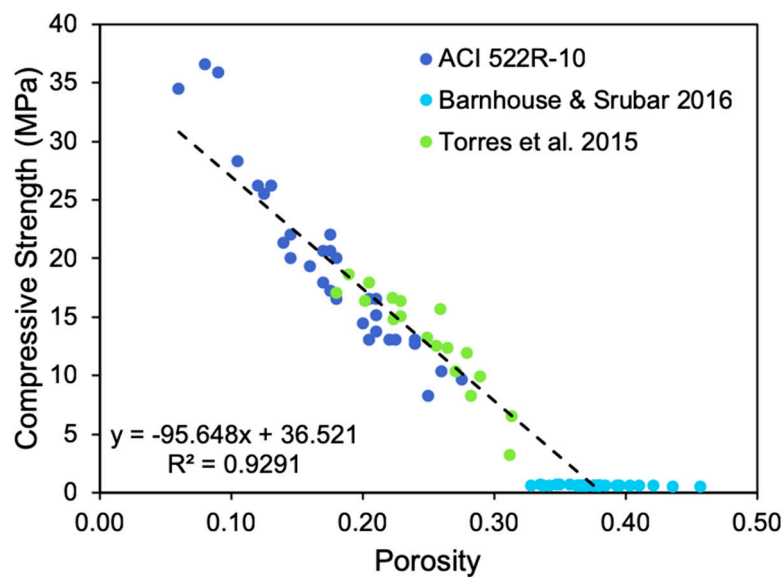


**Figure 1.** Relationship between compressive strength and porosity [4,10,38].

$$f'_c [MPa] = -95.65 * \varphi + 36.52 \tag{9}$$

where the porosity,  $\varphi$ , is in decimal form (between 0.1 and 0.4). Similarly, a modified form of the Carman-Kozeny model [37] is used to calculate the hydraulic conductivity from porosity:

$$K \left[ \frac{cm}{s} \right] = \propto \left[ \frac{\varphi^3}{(1 - \varphi)^3} \right] \tag{10}$$

In Equation (10), the porosity,  $\varphi$ , is in percentage form. A standard  $\alpha$  value of 30 is used. Using the relationships defined above, the compressive strength and hydraulic conductivity of each pervious concrete mixture can be estimated, enabling analysis of trends in CO<sub>2</sub> sequestration potential with these important design parameters.

### 2.3. Lifecycle Assessment (LCA) Methodology

The LCA performed in this study followed the ISO 14040/14044 standard, including lifecycle stages A1–A3 and B1 as specified in EN 15804. The following sections define the LCA goal and scope, life cycle inventory (LCI) analysis, environmental impact assessment, and limitations of the study.

#### 2.3.1. Goal and Scope Definition

This screening LCA investigated the net CO<sub>2</sub> equivalent emissions (CO<sub>2</sub>e) emissions of pervious concrete mixtures with w/c ratios of 0.25, 0.30, and 0.35 that have porosities ranging from 15% to 30%. The environmental impact reported has a global warming potential (kg CO<sub>2</sub>e) for each mix design, as summarized in Table 2. The results of the LCA were used to compare initial cradle-to-gate CO<sub>2</sub> emissions—more specifically CO<sub>2</sub>e, which accounts for the global warming potential of other greenhouse gases, including methane and nitrous oxide—to the amount of CO<sub>2</sub> recoverable during the use phase as calculated by the previously derived mathematical model.

The system boundary used for initial CO<sub>2</sub>e emissions was raw material supply (A1), transportation (A2), manufacturing (A3), while the system boundary for recoverable CO<sub>2</sub> is the use phase (B1). The transportation stage (A4) and the construction stage (A5) were not included in the analysis.

The declared unit considered in this LCA was a 1 m<sup>3</sup> of pervious concrete. As discussed in Section 2.1.5, 100% of the cement paste in each pervious concrete mixture is assumed to carbonate, due to its thin thickness relative to the depth of carbonation. Because 100% of the cement paste is assumed to carbonate, the declared unit is the same as the functional unit for the scope of this LCA since the geometry has no impact on the rate of carbonation.

#### 2.3.2. Lifecycle Inventory (LCI) Data

Athena Impact Estimator for Buildings (IE4B) (v5.2) was used to calculate the cradle-to-gate emissions of each pervious concrete mix design. Athena IE4B is an industry-tested whole-building lifecycle assessment tool that is commonly used to perform LCAs of whole buildings and individual building components. The LCI that Athena IE4B uses for assessing environmental impacts is regionally sensitive, and all data is typically less than 10 years old.

The User Defined Concrete Mix Design Library tool within Athena IE4B was used to input each mix design considered for the USA region. The initial cradle-to-gate CO<sub>2</sub> emissions (kg CO<sub>2</sub>e) for a declared unit (1 m<sup>3</sup>) of each mix design were calculated by the software. The cradle-to-gate environmental impacts for each mix design were compared to the recoverable CO<sub>2</sub> for each concrete volume, as described in Section 2.1.

#### 2.3.3. Limitations of the Study

- As a screening LCA, emissions associated with construction and transportation (A4 and A5) were not considered. Only lifecycle stages A1–A3 and B1 were included in the scope of this study. To perform a complete LCA specific to a building project using pervious concrete, these stages should be included in the system boundary.
- Only CH (i.e., portlandite) was considered to carbonate in the model used by this study. While other calcium silicate phases also have the potential to carbonate (as discussed), thus it is conservative to not consider their CO<sub>2</sub> uptake.

- This study assumed that all cement paste carbonates fully to report a conservative theoretical maximum. It has been shown that the actual degree of carbonation is less than 1.0 and may likely vary from 0.2 to 0.7 as previously discussed.
- Due to limitations in IE4B, aggregate size was not differentiated in the formulation of the mix designs in the *User Defined Concrete Mix Design Library*. While different aggregate sizes require different manufacturing processes, for this study, “Coarse Aggregate Natural” was used as the input for the IE4B software. It is expected that smaller aggregate sizes will require a marginal increase in manufacturing emissions, but are ignored in this study.

### 3. Results and Discussion

#### 3.1. Initial CO<sub>2</sub>e Emissions

Figure 2 summarizes the initial cradle-to-gate CO<sub>2</sub>e emissions for a declared 1 m<sup>3</sup> of each pervious concrete mixture analyzed herein. Expectedly, as the w/c ratio increases, initial CO<sub>2</sub>e emissions decrease due to lower cement content. For instance, for each unique porosity and aggregate size combination, the emissions of the w/c = 0.25 mixtures are approximately 17% larger than the w/c = 0.35 mixtures. In addition, increasing the porosity reduces the cradle-to-gate CO<sub>2</sub>e emissions. This trend is also expected, since higher-porosity mixtures have more void space and, therefore, contain less cement per unit volume. For example, each 1 m<sup>3</sup> of pervious concrete with 15% porosity and a w/c = 0.30 emits 204 kg CO<sub>2</sub>e more than the 30% porosity mixture with the same w/c ratio. In fact, the initial CO<sub>2</sub>e emissions of the 15% porosity mixtures are 51% larger than those of the 30% porosity mixtures for the 0.25 w/c ratio considered herein. A similar magnitude difference was observed for the other w/c ratios. The mixture with a w/c = 0.25 and porosity of 15% generates the highest initial CO<sub>2</sub>e emissions (659 kg CO<sub>2</sub>e/m<sup>3</sup>), while the mixture with a w/c = 0.35 and porosity of 30% generates the least (374 kg CO<sub>2</sub>e/m<sup>3</sup>).

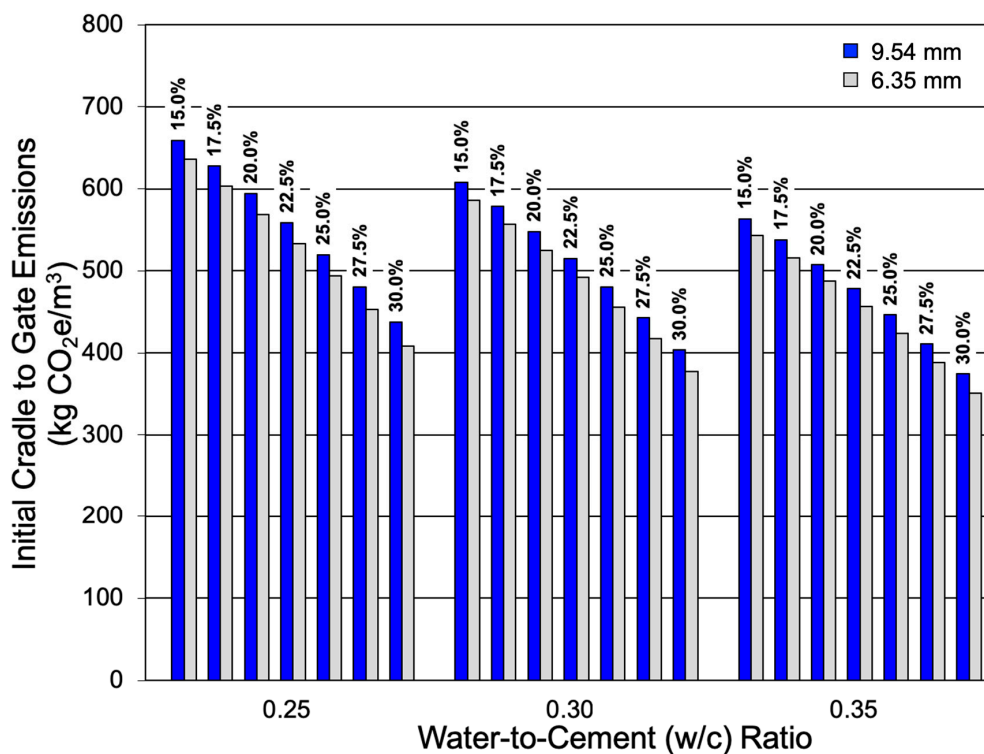
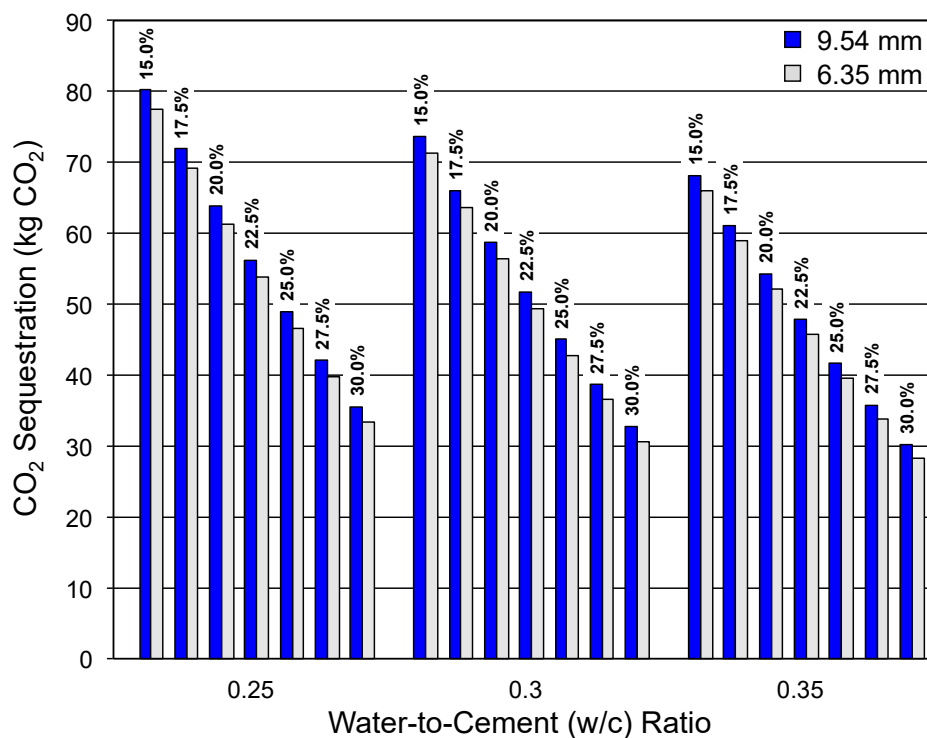


**Figure 2.** Initial cradle-to-gate CO<sub>2</sub>e emissions of pervious concrete mixtures designed according to the NRMCA design methodology [35,36]. Design porosity of each mixture is indicated above its respective column. Aggregate size is differentiated by color.

### 3.2. CO<sub>2</sub> Sequestration Potential

#### 3.2.1. Effect of w/c Ratio

Figure 3 shows the effect of w/c ratio on the estimated CO<sub>2</sub> sequestration potential of 1 m<sup>3</sup> of pervious concrete for the aggregate types and porosities listed in Table 2. Expectedly, as w/c ratio increases for a given design porosity, the CO<sub>2</sub> sequestration potential decreases. For example, a mixture with 9.54 mm aggregate, 15% porosity, and a w/c = 0.25 will sequester approximately 17.6% more CO<sub>2</sub> than a mixture with an identical aggregate size and porosity but a w/c = 0.35. This reduction in CO<sub>2</sub> sequestration potential is again attributable to the decreased cement content per unit volume of mixtures with lower w/c ratios.



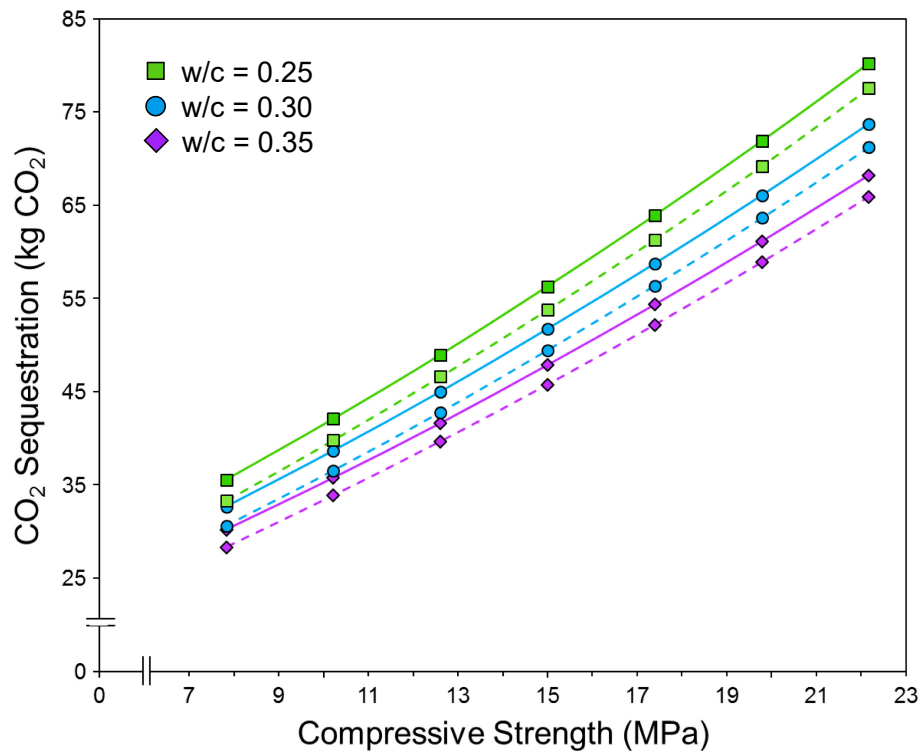
**Figure 3.** CO<sub>2</sub> sequestration potential for 1 m<sup>3</sup> of pervious concrete. Design porosity of each mixture is indicated above its respective column. Aggregate size is differentiated by color.

Figure 3 also demonstrates that, for a given w/c ratio, CO<sub>2</sub> sequestration potential decreases with increasing porosity. This result was also anticipated, as decreased cement content corresponds to thinner average cementitious paste thicknesses around aggregates within the pervious concrete matrix [10]. For mixtures with equivalent w/c ratios and design porosities, the use of smaller aggregate results in lower CO<sub>2</sub> sequestration potentials as compared to the use of a larger aggregate (Figure 3). The cementitious paste thickness for small aggregate mixtures is, on average, less than a large aggregate mixture of equivalent porosity [10,39]. Thus, the total cement content in small-aggregate mixtures will be lower compared to large-aggregate mixtures with the same design porosity. Due to the decreased quantity of cement, and thus CH content, the in situ CO<sub>2</sub> sequestration potential also decreases. As an example, mixtures designed for 30% porosity exhibit a 6.8% difference in CO<sub>2</sub> sequestration potential between mixtures that use smaller versus larger aggregate sizes.

#### 3.2.2. Effect of Compressive Strength

Figure 4 illustrates the effect of compressive strength on the CO<sub>2</sub> sequestration potential of 1 m<sup>3</sup> of pervious concrete designed according to the mixture proportions presented in Table 2. For the intermediate w/c ratio of 0.30, the highest compressive strength mixture (22.2 MPa) exhibits a CO<sub>2</sub>

sequestration potential 2.4 times greater than the lowest compressive strength mixture (7.8 MPa). As the compressive strength for a pervious concrete mixture design increases, higher cement contents are required, resulting in a higher CO<sub>2</sub> sequestration potential compared to lower-strength mixtures. For normal concrete mixtures, previous work has also substantiated the relationship between higher cement content and higher in situ CO<sub>2</sub> sequestration for a given volume of concrete [28].



**Figure 4.** Effect of compressive strength on the CO<sub>2</sub> sequestration potential of 1 m<sup>3</sup> of pervious concrete with varying water-to-cement (w/c) ratios and both 9.35 mm (—) and 6.35 mm (- - -) aggregate.

Furthermore, Figure 4 demonstrates that mixtures containing larger coarse aggregates result in higher CO<sub>2</sub> sequestration potentials for a given compressive strength. At the lowest compressive strength, mixtures containing 9.54 mm coarse aggregate have CO<sub>2</sub> sequestration potentials 3.5% greater than equivalent 6.35 mm coarse aggregate mixtures for all w/c ratios. Similarly, at the highest compressive strength, the CO<sub>2</sub> sequestration potential of 9.54 mm aggregate mixtures is 6.8% larger. As previously discussed, to achieve a desired compressive strength, large-aggregate mixtures require increased cement content as compared to small-aggregate mixtures, thereby increasing the potential for in situ CO<sub>2</sub> sequestration.

Similar to Figure 3, Figure 4 indicates that, as w/c ratio increases, CO<sub>2</sub> sequestration potential decreases. Figure 4 additionally demonstrates that the effect of varying w/c ratio on CO<sub>2</sub> sequestration potential is more pronounced at higher design compressive strengths. At all compressive strengths, a 9.54 mm mixture with a w/c = 0.35 exhibits a CO<sub>2</sub> sequestration potential 17.6% greater than a mixture with a w/c = 0.25. At the highest compressive strength, this difference is 85.4 kg CO<sub>2</sub>, while the difference is 46.3 kg CO<sub>2</sub> at the lowest compressive strength. In this model, compressive strength is calculated only as a function of porosity using the relationship developed in Figure 1, and thus variations in w/c do not have an effect on compressive strength.

### 3.2.3. Effect of Design Porosity and Hydraulic Conductivity

Figure 5a demonstrates that CO<sub>2</sub> sequestration potential decreases almost linearly with increasing design porosity. For instance, the decrease in CO<sub>2</sub> sequestration potential for an increase in porosity from 15% to 17.5% is 7.7 kg CO<sub>2</sub> for 9.54 mm aggregate mixtures. This difference is marginally larger

than the difference between 27.5% and 30% porosity for 9.54 mm aggregate mixtures, which differ in CO<sub>2</sub> sequestration potential by approximately 6.0 kg CO<sub>2</sub>. While mixtures exhibit a slight decrease in the rate of change of CO<sub>2</sub> sequestration potential with increases in bulk porosity, a linear regression of the relationship between sequestration potential and porosity results in an R<sup>2</sup> = 0.998, indicating a near-linear relationship. Further, the standard deviation decreases as design porosity increases due to the guidelines of ACI 522R [4], indicating that the variation in CO<sub>2</sub> sequestration potential between w/c = 0.25 and w/c = 0.35 mixtures decreases with increases in porosity. This finding is consistent with the trends exhibited in Figure 4.

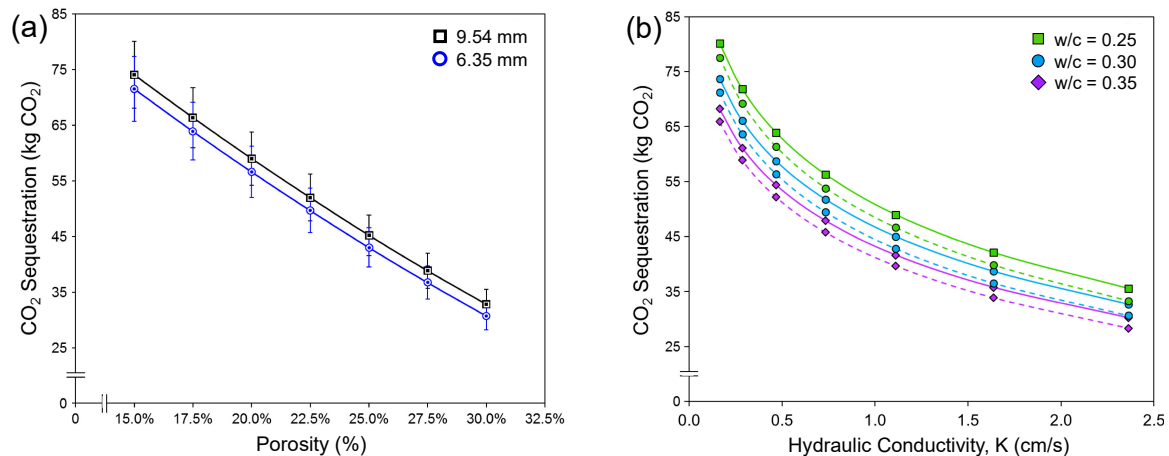


**Figure 5.** (a) Effect of design porosity on average CO<sub>2</sub> sequestration of 1 m<sup>3</sup> of pervious concrete. Means and error bars represent ± one standard deviation of CO<sub>2</sub> sequestration potential from fixed-porosity mixtures designed using water-to-cement (w/c) ratios of 0.25, 0.30, and 0.35. Aggregate size is differentiated by color. (b) Effect of design hydraulic conductivity on average CO<sub>2</sub> sequestration potential of a 1 m<sup>3</sup> of pervious concrete, with varying w/c ratios and both 9.35 mm (—) and 6.35 mm (---) aggregate.

A two-tail standard t-test assuming nonequivalent variances was conducted to determine the significance of the effect of aggregate size on CO<sub>2</sub> sequestration potential. The null hypothesis predicts a zero difference between means of the two aggregate size mixture design samples. Using an α-parameter value of 0.05,  $p = 0.61$ , failing to reject the null hypothesis. Thus, based on this analysis, the mixture designs considered herein give no indication that aggregate size has a significant effect on CO<sub>2</sub> sequestration potential.

Figure 5b demonstrates that increasing the design hydraulic conductivity of a mixture results in decreasing CO<sub>2</sub> sequestration potential. Hydraulic conductivity is directly related to porosity, as a more porous concrete matrix enables faster permeation. Thus, similar to porosity, increasing hydraulic conductivity requires decreased cement paste thicknesses. Figure 5b also illustrates the trend of increasing deviation between mixtures of different w/c ratios. In the case of hydraulic conductivity, otherwise equivalent mixtures with w/c ratios of 0.25 and 0.35 exhibit the largest difference in sequestration potential at the lowest hydraulic conductivity.

Aggregate shape (angular vs. rounded) has a significant impact on the porosity of pervious concrete and, hence, the CO<sub>2</sub> sequestration potential. More angular aggregates require more water in normal concrete to achieve the same workability as round aggregates and, for pervious concrete, the use of angular aggregates result in more porous mixtures [40,41]. While this study does not explicitly consider differences in aggregate type in the mixture designs or the analyses that ensue, it is expected that the use of more angular aggregates for the same target design porosity will result in only minor reductions in porosity and, therefore, impart trivial reductions on the CO<sub>2</sub> sequestration potential.

### 3.3. Net Lifecycle (and Recoverable) CO<sub>2</sub> Emissions

Net CO<sub>2</sub>e emissions for 1 m<sup>3</sup> of each pervious concrete mixture were calculated by subtracting the CO<sub>2</sub> sequestration potential discussed in Section 3.2 from the initial cradle-to-gate CO<sub>2</sub>e emissions discussed in Section 3.1. The results are summarized in Figure 6. As previously noted in Section 2.1.5, the CO<sub>2</sub> sequestration potential assumes full carbonation of CH phases and represents the theoretical upper bound. Therefore, calculations of net emissions incorporate maximum CO<sub>2</sub> sequestration potential with the conservative assumptions stated herein.

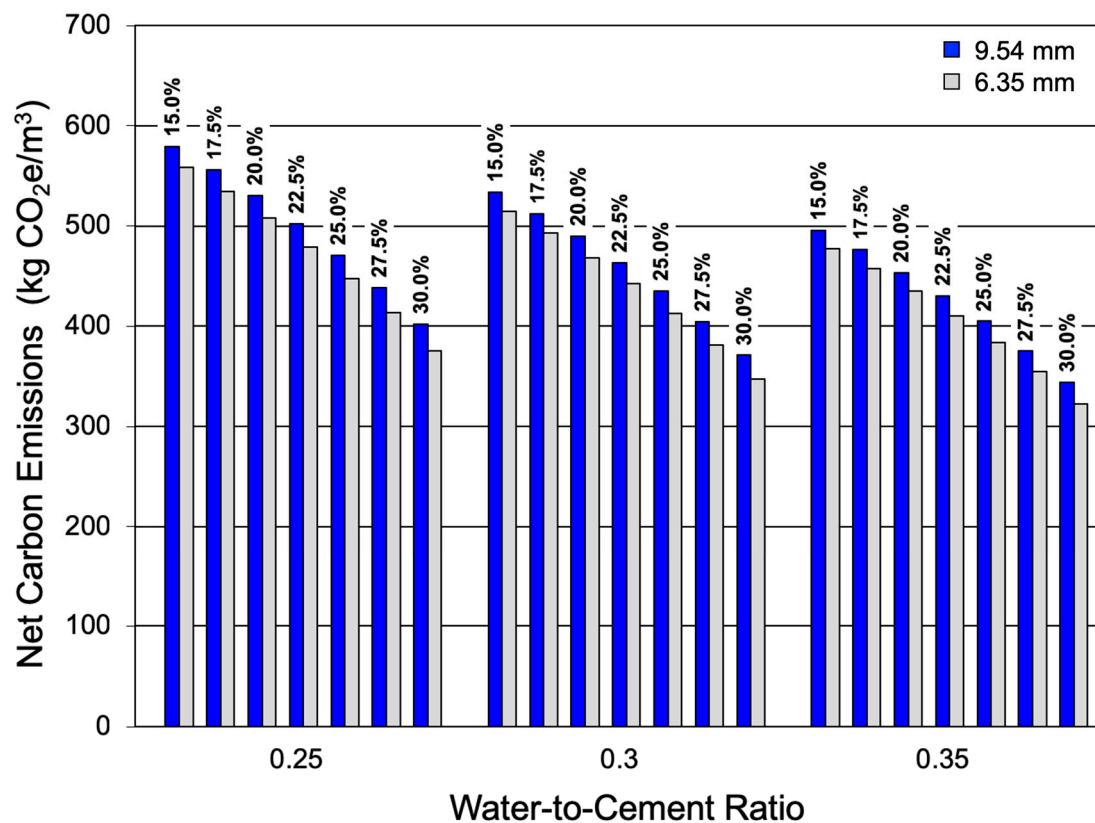


Figure 6. Net CO<sub>2</sub>e emissions of 1 m<sup>3</sup> of pervious concrete. Design porosity of each mixture is indicated above its respective column. Aggregate size is differentiated by color.

Figure 6 demonstrates that mixtures with higher cement contents correspond to larger CO<sub>2</sub>e emissions despite increased CO<sub>2</sub> sequestration potential. As anticipated, pervious concrete mixtures with lower compressive strengths and, hence, lower cement contents, result in lower initial global warming potentials (Figure 4). For example, given that cement content decreases with increasing w/c ratio and increasing porosity, the net CO<sub>2</sub>e emissions for mixtures with w/c = 0.25 are 17% greater than mixtures with w/c = 0.35 for all porosities. For equivalent w/c ratios, mixtures with 15% porosity result in 44% more CO<sub>2</sub>e emissions than mixtures with 30% porosity. As discussed in Section 3.2, increased porosity correlates to decreased compressive strength. Therefore, net CO<sub>2</sub>e emissions are lower for mixtures exhibiting lower compressive strength. Similarly, as discussed in Section 3.3, increasing porosity correlates to increasing hydraulic conductivity. Thus, net CO<sub>2</sub>e emissions are lower for mixtures with higher hydraulic conductivity.

Table 3 displays the percentage of initial emissions associated with each pervious concrete mixture that is recoverable by CO<sub>2</sub> sequestration. These data elucidate that lower porosity mixtures recover larger fractions of initial emissions. Further, Table 3 indicates that w/c ratio and aggregate size have negligible effects on the fraction of recoverable CO<sub>2</sub> emissions. Because the model assumes full carbonation of CH, potential differences in the rate of carbonation between these mixtures are

obfuscated by the assumption that all paste carbonates within the design service life. In reality, however, mixtures with lower w/c ratios and lower porosities (higher cement content) will, in theory, reach full carbonation at a slower rate due to thicker aggregate coating [3,10,17]. As design porosity increases, the fraction of initial emissions from cement production decreases, thereby reducing the fraction of emissions recoverable via CO<sub>2</sub> sequestration. Likewise, the fraction of overall emissions that carbonation can recover is reduced with decreasing compressive strength and increasing hydraulic conductivity.

**Table 3.** Percentage of initial emissions recoverable via CO<sub>2</sub> sequestration for 1 m<sup>3</sup> of pervious concrete.

Design Porosity	Aggregate Size (mm)		w/c = 0.25		w/c = 0.30		w/c = 0.35	
	9.54	6.35	9.54	6.35	9.54	6.35	9.54	6.35
15.0	12.17%	12.19%	12.14%	12.16%	12.11%	12.12%		
17.5	11.45%	11.47%	11.42%	11.44%	11.37%	11.40%		
20.0	10.75%	10.77%	10.71%	10.74%	10.71%	10.71%		
22.5	10.07%	10.09%	10.05%	10.06%	10.01%	10.03%		
25.0	9.42%	9.43%	9.37%	9.40%	9.32%	9.36%		
27.5	8.76%	8.79%	8.73%	8.75%	8.71%	8.71%		
30.0	8.13%	8.15%	8.10%	8.11%	8.07%	8.07%		

It is well known that incorporation of SCMs, such as fly ash and slag, in pervious concrete mixtures can reduce the initial cradle-to-gate CO<sub>2</sub> emissions but also alter the CO<sub>2</sub> sequestration potential. Previous studies concerning the impact of SCMs on CO<sub>2</sub> sequestration for regular concrete mixtures indicate that CO<sub>2</sub> sequestration potential ( $C_m$ ) linearly decreases as % replacement by SCM increases [28]. Given that OPC is used as the binder in both regular and pervious concrete mixtures, the same set of chemical reactions occur, indicating that CO<sub>2</sub> sequestration potential in pervious concrete mixtures would also decrease with increased cement replacement by SCMs. Therefore, the inclusion of SCMs in pervious concrete mixtures would result in decreased initial CO<sub>2</sub> emissions in addition to decreased CO<sub>2</sub> sequestration potential. While CO<sub>2</sub> sequestration potential would decrease in these circumstances, net CO<sub>2</sub> emissions would also likely decrease [19], indicating that SCM use in pervious concrete should be encouraged from a net-emissions standpoint.

As previously discussed, the fraction of initial emissions recoverable via carbonation has been previously studied for regular OPC concrete mixtures [19,20,25,40]. For both regular and pervious concrete mixtures, the amount of sequesterable CO<sub>2</sub> increases as compressive strength increases [40]. Results from [40] indicate that normal Type I OPC mixtures with compressive strengths of 15 MPa can sequester up to 16.8% of their initial CO<sub>2</sub>e emissions, while mixtures with compressive strengths of 45 MPa can recover approximately 17.1% through sequestration. Therefore, typical concrete elements have the ability to recover a larger fraction of initial emissions via complete carbonation of available CH than pervious concrete elements, which are predicted herein to recover approximately 8–12% of initial emissions. However, as previously discussed, the rates at which the carbonation process occurs are different in normal versus pervious concrete due the bulk porosity and air and water permeability of pervious concrete. Therefore, a pervious concrete would achieve full carbonation faster than a normal concrete with similar cement contents per unit volume.

In summary, this study elucidates that, for both regular and pervious concrete mixtures, lower initial CO<sub>2</sub> emissions correspond to lower net CO<sub>2</sub> emissions, even when carbonation is included in the carbon accounting. Concrete mixtures with higher cement contents exhibit higher CO<sub>2</sub> sequestration potentials. However, increased CO<sub>2</sub> sequestration potential is outweighed by increased initial CO<sub>2</sub> emissions, which result in higher net lifecycle emissions for concrete mixtures with higher cement contents. Therefore, as was also concluded in [19] for normal OPC concrete, minimizing initial CO<sub>2</sub> emissions when designing concrete mixtures—for either normal or pervious concrete—rather than maximizing in situ CO<sub>2</sub> sequestration potential is a most beneficial strategy to minimize net overall CO<sub>2</sub> emissions.

#### 4. Conclusions

The formulation of a mathematical model for quantifying the in situ CO<sub>2</sub> sequestration potential of pervious concrete mixtures was presented and implemented herein. The model was derived from OPC hydration and carbonation reactions and was implemented for 42 pervious concrete mixtures that varied in aggregate size (6.35 and 9.54 mm), water-to-cement (w/c) ratio (0.25, 0.30, 0.35), and design porosity (15–30%). Additionally, initial cradle-to-gate CO<sub>2</sub>e emissions of each concrete mixture were quantified using a screening LCA, enabling quantification of the percentage of initial CO<sub>2</sub> emissions recoverable through in situ CO<sub>2</sub> sequestration. Results elucidate the following main conclusions of this study:

- The maximum amount of initial CO<sub>2</sub> emissions of pervious concrete that can be recovered through CO<sub>2</sub> sequestration is estimated to be approximately 12%.
- Higher w/c ratios, design porosities, and hydraulic conductivities correspond to decreased CO<sub>2</sub> sequestration potential, while higher compressive strength corresponds to higher CO<sub>2</sub> sequestration potential. Aggregate size imparts a negligible effect.
- LCA results indicate that net CO<sub>2</sub>e emissions decline with increases in w/c ratio, design porosity, and hydraulic conductivity, while increased cement content increases both CO<sub>2</sub> sequestration potential and, to a greater extent, initial CO<sub>2</sub>e emissions.
- Mixtures with higher cement contents always exhibit higher net CO<sub>2</sub>e emissions despite their increased CO<sub>2</sub> sequestration potential.

The model presented here may be implemented by design engineers and architects in LCAs to make more informed decisions concerning the environmental impacts of pervious concrete in building and infrastructure applications. LCAs enable environmental impacts, such as global warming potential, to be considered in materials design, permitting engineers and architects the ability to reduce and avoid excess CO<sub>2</sub> emissions. As illustrated herein, while LCA studies that negate in situ carbonation may be over-estimating the cradle-to-gate CO<sub>2</sub> emissions of pervious concrete up to ≈ 12%, avoidance of initial CO<sub>2</sub> emissions is a more advantageous strategy than relying on the carbonation process to recover a meaningful quantity of initial CO<sub>2</sub> emissions.

**Author Contributions:** Conceptualization, W.V.S. III; Formal analysis, E.E., J.H.A., and W.V.S. III; Funding acquisition, W.V.S. III; Investigation, E.E. and J.H.A.; Methodology, E.E., J.H.A., and W.V.S. III; Project administration, W.V.S. III; Resources, W.V.S. III; Supervision, J.H.A. and W.V.S. III; Validation, J.H.A.; Visualization, E.E. and J.H.A.; Writing—original draft, E.E. and J.H.A.; Writing—review & editing, W.V.S. III.

**Funding:** This research was funded by the Discovery Learning Apprenticeship at the University of Colorado Boulder.

**Acknowledgments:** This research was made possible by the Department of Civil, Environmental, and Architectural Engineering, the College of Engineering and Applied Sciences, the Living Materials Laboratory, and the Discovery Learning Apprenticeship Program at the University of Colorado Boulder. This work represents the views of the authors and not necessarily those of the sponsors.

**Conflicts of Interest:** The authors declare no conflict of interest. The funders had no role in the design of the study; in the collection, analyses, or interpretation of data; in the writing of the manuscript, or in the decision to publish the results.

#### References

1. Poh, S.; Zhao, P.; Chen, C.; Goh, Y.; Adebayo, H.; Hung, K.; Wah, C. Characterization of pervious concrete with blended natural aggregate and recycled concrete aggregates. *J. Clean. Prod.* **2018**, *181*, 155–165.
2. Carsana, M.; Tittarelli, F.; Bertolini, L. Use of no-fines concrete as a building material: Strength, durability properties and corrosion protection of embedded steel. *Cem. Concr. Res.* **2013**, *48*, 64–73. [[CrossRef](#)]
3. Tamai, M.; Mizuguchi, H.; Hatanaka, S.; Katahira, H.; Nakazawa, T.; Yanagibashi, K.; Kunieda, M. Design, construction and recent applications of porous concrete in Japan. In *Proceedings of the JCI Symposium on Design, Construction, and Recent Applications of Porous Concrete*; Japan Concrete Institute: Tokyo, Japan, 2004.

4. American Concrete Institute (ACI). *ACI 522R-10: Report on Pervious Concrete*; American Concrete Institute (ACI): Farmington Hills, MI, USA, 2010; Volume 10.
5. Welker, A.L.; Barbis, J.D.; Jeffers, P.A. A side-by-side comparison of pervious concrete and porous asphalt. *J. Am. Water Resour. Assoc.* **2012**, *48*, 809–819. [[CrossRef](#)]
6. Haselbach, L.; Boyer, M.; KeVERN, J.; Schaefer, V. Cyclic heat island impacts on traditional versus pervious concrete pavement systems. *Transp. Res. Rec. J. Transp. Res. Board* **2011**, *2240*, 107–115. [[CrossRef](#)]
7. Horst, M.; Welker, A.L.; Traver, R. Multiyear performance of a pervious concrete infiltration basin BMP. *J. Irrig. Drain. Eng.* **2011**, *137*, 352–358. [[CrossRef](#)]
8. Nemirovsky, E.M.; Welker, A.L.; Lee, R. Quantifying evaporation from pervious concrete systems: Methodology and hydrologic perspective. *J. Irrig. Drain. Eng.* **2012**, *139*, 271–277. [[CrossRef](#)]
9. Kwiatkowski, M.; Welker, A.L.; Traver, R.G.; Vanacore, M.; Ladd, T. Evaluation of an infiltration best management practice utilizing pervious concrete. *J. Am. Water Resour. Assoc.* **2008**, *43*, 1208–1222. [[CrossRef](#)]
10. Torres, A.; Hu, J.; Ramos, A. The effect of the cementitious paste thickness on the performance of pervious concrete. *Constr. Build. Mater.* **2015**, *95*, 850–859. [[CrossRef](#)]
11. Neithalath, N.; Sumanasooriya, M.S.; Deo, O. Characterizing pore volume, sizes, and connectivity in pervious concretes for permeability prediction. *Mater. Charact.* **2010**, *61*, 802–813. [[CrossRef](#)]
12. Huang, B.; Wu, H.; Shu, X.; Burdette, E.G. Laboratory evaluation of permeability and strength of polymer-modified pervious concrete. *Constr. Build. Mater.* **2010**, *24*, 818–823. [[CrossRef](#)]
13. Zhong, R.; Wille, K. Compression response of normal and high strength pervious concrete. *Constr. Build. Mater.* **2016**, *109*, 177–187. [[CrossRef](#)]
14. Huntzinger, D.N.; Eatmon, T.D. A life-cycle assessment of Portland cement manufacturing: Comparing the traditional process with alternative technologies. *J. Clean. Prod.* **2009**, *17*, 668–675. [[CrossRef](#)]
15. Worrell, E.; Price, L.; Martin, N.; Hendriks, C.; Meida, L.O. Carbon dioxide emissions from the global cement industry. *Carbon* **2001**, *26*, 303–329. [[CrossRef](#)]
16. Xi, F.; Davis, S.J.; Ciaes, P.; Crawford-Brown, D.; Guan, D.; Pade, C.; Shi, T.; Syddall, M.; Lv, J.; Ji, L.; et al. Substantial global carbon uptake by cement carbonation. *Nat. Geosci.* **2016**, *9*, 880–883. [[CrossRef](#)]
17. Pade, C.; Guimaraes, M. The CO<sub>2</sub> uptake of concrete in a 100 year perspective. *Cem. Concr. Res.* **2007**, *37*, 1348–1356. [[CrossRef](#)]
18. Gajda, J.; Miller, F.M. *Concrete as a Sink for Atmospheric Carbon Dioxide: A Literature Review and Estimation of CO<sub>2</sub> Absorption by Portland Cement Concrete*; Portland Cement Association: Skokie, IL, USA, 2000.
19. Yang, K.H.; Seo, E.A.; Tae, S.H. Carbonation and CO<sub>2</sub> uptake of concrete. *Environ. Impact Assess. Rev.* **2014**, *46*, 43–52. [[CrossRef](#)]
20. García-Segura, T.; Yepes, V.; Alcalá, J. Life cycle greenhouse gas emissions of blended cement concrete including carbonation and durability. *Int. J. Life Cycle Assess.* **2014**, *19*, 3–12. [[CrossRef](#)]
21. Souto-Martinez, A.; Delesky, E.A.; Foster, K.E.O.; Srubar, W.V. Accounting for the carbon sequestration potential of reinforced concrete in a whole-building life-cycle assessment. In *AEI 2017*; American Society of Civil Engineers: Reston, VA, USA, 2017; pp. 285–298.
22. Souto-Martinez, A.; Arehart, J.H.; Srubar, W.V. Cradle-to-gate CO<sub>2</sub>e emissions vs. in situ CO<sub>2</sub> sequestration of structural concrete elements. *Energy Build.* **2018**, *167*, 301–311. [[CrossRef](#)]
23. Ashraf, W. Carbonation of cement-based materials: Challenges and opportunities. *Constr. Build. Mater.* **2016**, *120*, 558–570. [[CrossRef](#)]
24. Papadakis, V.G.; Vayenas, C.G.; Fardis, M.N. Fundamental modeling and experimental investigation of concrete carbonation. *ACI Mater. J.* **1991**, *88*, 363–373.
25. Collins, F. Inclusion of carbonation during the life cycle of built and recycled concrete: Influence on their carbon footprint. *Int. J. Life Cycle Assess.* **2010**, *15*, 549–556. [[CrossRef](#)]
26. Lagerblad, B. *Carbon Dioxide Uptake during Concrete Life Cycle—State of the Art*; Nordic Innovation Centre: Oslo, Norway, 2006; Volume CBI 2005:2, ISBN 9197607002.
27. ASTM C150/C150M-18 Standard Specification for Portland Cement. *ASTM Int.* **2018**, 1–9.
28. Mehta, P.K. *Concrete Structure, Properties and Materials*. 1986. Available online: <https://trid.trb.org/view/273357> (accessed on 18 November 2017).
29. Souto-Martinez, A.; Delesky, E.A.; Foster, K.E.O.; Srubar, W.V. A mathematical model for predicting the carbon sequestration potential of ordinary Portland cement (OPC) concrete. *Constr. Build. Mater.* **2017**, *147*, 417–427. [[CrossRef](#)]

30. Haselbach, L.M.; Liu, L. Calcium hydroxide formation in thin cement paste exposed to air. *ACI Mater. J.* **2010**, *107*, 365–371.
31. Golroo, A.; Tighe, S.L. Pervious concrete pavement performance modeling using the bayesian statistical technique. *J. Transp. Eng.* **2012**, *138*, 603–609. [[CrossRef](#)]
32. Engelsen, C.J.; Justnes, H.; Rønning, A.R. The quantity of CO<sub>2</sub> bound by concrete carbonation in Norway. In Proceedings of the Fourth International Conference on Sustainable Construction Materials and Technologies, Las Vegas, NV, USA, 7–11 August 2016.
33. Fridh, K.; Lagerblad, B. Carbonation of indoor concrete: Measurements of depths and degrees of carbonation. *Lund* **2013**. Available online: <https://lup.lub.lu.se/search/publication/4390005> (accessed on 18 November 2017).
34. Thiery, M.; Dangla, P.; Belin, P.; Habert, G.; Roussel, N. Carbonation kinetics of a bed of recycled concrete aggregates: A laboratory study on model materials. *Cem. Concr. Res.* **2013**, *46*, 50–65. [[CrossRef](#)]
35. Van Balen, K. Carbonation reaction of lime, kinetics at ambient temperature. *Cem. Concr. Res.* **2005**, *35*, 647–657. [[CrossRef](#)]
36. National Ready Mixed Concrete Association (NRMCA) Pervious Concrete: Guideline to Mixture Proportioning. Available online: <https://my.nrmca.org/Main/ItemDetail?iProductCode=2PE001> (accessed on 18 November 2017).
37. Barnhouse, P.W.; Srubar, W.V. Material characterization and hydraulic conductivity modeling of macroporous recycled-aggregate pervious concrete. *Constr. Build. Mater.* **2016**, *110*, 89–97. [[CrossRef](#)]
38. Torres, A.; Gaedicke, C.; Hu, J.; Bejugam, R.; Mcmasters, S. Comparing Design Void Content with Actual Void Content of Laboratory Prepared Pervious Concrete. *Mater. Sci. Appl.* **2018**, *9*, 596–613.
39. Joshaghani, A.; Ramezani pour, A.A.; Ataei, O.; Golroo, A. Optimizing pervious concrete pavement mixture design by using the Taguchi method. *Constr. Build. Mater.* **2015**, *101*, 317–325. [[CrossRef](#)]
40. Zhang, Z.; Zhang, Y.; Yan, C.; Liu, Y. Influence of crushing index on properties of recycled aggregates pervious concrete. *Constr. Build. Mater.* **2017**, *135*, 112–118. [[CrossRef](#)]
41. Tennis, P.D.; Leming, M.L.; Akers, D.J. *Pervious Concrete Pavements*; EB302.02; Portland Cement Association: Skokie, IL, USA, 2004; ISBN 0893122424.



© 2019 by the authors. Licensee MDPI, Basel, Switzerland. This article is an open access article distributed under the terms and conditions of the Creative Commons Attribution (CC BY) license (<http://creativecommons.org/licenses/by/4.0/>).